Robust single-molecule approach for counting autofluorescent proteins

Laurent Cognet[*,†]
Catherine Tardin[†,‡]
Marie-Laure Martin Négrier
Université Bordeaux
Centre de Physique Moléculaire Optique et Hertzienne
Centre National de la Recherche Scientifique
351 Cours de la Libération
33405 Talence, France

Christelle Breillat
Françoise Coussen
Daniel Choquet
Université Bordeaux
Laboratoire de Physiologie Cellulaire de la Synapse
Centre National de la Recherche Scientifique
Institut François Magendie
1 rue Camille Saint-Saëns
33077 Bordeaux, France

Brahim Lounis
Université Bordeaux
Centre de Physique Moléculaire Optique et Hertzienne
Centre National de la Recherche Scientifique
351 Cours de la Libération
33405 Talence, France

Abstract. Using single-molecule microscopy, we present a method to quantify the number of single autofluorescent proteins when they cannot be optically resolved. This method relies on the measurement of the total intensity emitted by each aggregate until it photobleaches. This strategy overcomes the inherent problem of blinking of green fluorescent proteins. In the case of small protein aggregates, our method permits us to describe the mean composition with a precision of one protein. For aggregates containing a large number of proteins, it gives access to the average number of proteins gathered and a signature of the inhomogeneity of the aggregates' population. We applied this methodology to the quantification of small purified citrine multimers. © *2008 Society of Photo-Optical Instrumentation Engineers.* [DOI: 10.1117/1.2940600]

Keywords: autofluorescent proteins; green fluorescent protein; single molecule; protein stoechiometry; fluorescence.

Paper 07260SSR received Jul. 16, 2007; revised manuscript received Sep. 24, 2007; accepted for publication Nov. 4, 2007; published online Jun. 23, 2008.

1 Introduction

The understanding of biological phenomena requires a quantitative knowledge of the cellular compartments and structures that are studied. In particular, their molecular composition drives the molecular mechanisms involved in their functions and must be known with precision. One of the most promising techniques to investigate molecular events in living cells at the subcellular level is single-molecule microscopy.[1–5] Different attempts based on the single-molecule technique have already been performed to measure the stochiometry of an assembly of biomolecules.[6–8] It was proposed to use the antibunching phenomenon signature of a low number of emitters.[8] However, the use of this method is limited to the study of small aggregates, and because of its high sensitivity to the background, it cannot be used in living cells. It was also thought to evaluate the stochiometry of different proteins likely to aggregate at the membrane surface by measuring the intensity emitted and detected by the assemblies in given image frames.[6,7] In these studies, the fluorescent markers used to label the proteins were mutants of the green fluorescent protein (GFP), and because of the nonideal photophysical properties of the GFPs, these attempts failed to offer a reliable way to access the stochiometry of molecular assemblies.[9,10] Another elegant strategy could rely on the use of serial photoactivation and subsequent bleaching of numerous sparse subsets of photoactivatable fluorescent protein molecules.[5] However, this method is not readily applicable to living systems since it needs long imaging sequences and is therefore limited to fixed samples. It also requires rather sophisticated instrumentation and analysis.

The method proposed here is also based on the use of a GFP mutant and single-molecule microscopy. Autofluorescent proteins were chosen for their simplicity to obtain a one-to-one labeling ratio of the proteins of interest. This method relies on the measurement of the total number of counts emitted from an aggregate of fluorescent proteins, which constitutes a robust and simple strategy to obtain the precise composition of small assemblies and a good approximation of the composition of larger aggregates.

2 Materials and Methods

2.1 *Trimers Production and Purification*

Trimers were based on fibronectin-tenascin domains (FN-TN) construction[11] by replacing the nucleotides' coding for the FN fragment placed at the N-terminus by the ones coding for citrine, a mutant of enhanced GFP (eGFP).[14] Plasmids were transformed into E. coli BL21(DE3)strains, the bacteria were grown until the culture reached an optical density (OD) of 0.7

[†]These authors contributed equally to this work.
[‡]Present address: Institut de Pharmacologie et Biologie Structurale, UMR CNRS 5089, 205, route de Narbonne, 31077 Toulouse cedex, France.
*Address all correspondence to Laurent Cognet, Centre de Physique Moléculaire Optique et Hertzienne, Université Bordeaux 1 & CNRS, 351 Cours de la Libération, 33405 Talence, France; Tel: +33 (0)5 4000 6212; E-mail: lcognet@u-bordeaux1.fr

1083-3668/2008/13(3)/031216/5/$25.00 © 2008 SPIE

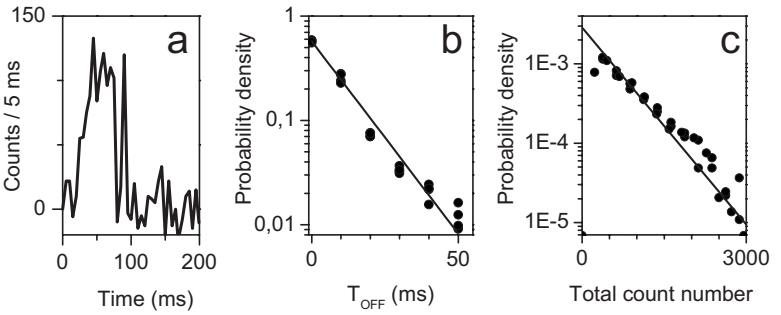

Fig. 1 (a) Typical example of an intensity trace detected from a single citrine. (b) Distribution of the duration of the initial dark state measured on 2052 individual citrine molecules (dots). The distribution is fitted by an exponential function (solid line) with a characteristic time equal to 11 ± 1 ms. (c) Distribution of the total count number detected from individual molecules until complete photobleaching ($n=2721$ molecules).

at A600, and protein expression was induced by adding 0.4 mM isopropyl-beta-D-thiogalactopyranoside (IPTG) over three hours. The bacteria were suspended in buffer [100 mM NaCl, 50 mM Tris pH 8.0, 1 mM ethylene diamine tetraacetic acid (EDTA)] and lysed with lysozyme (0.2 mg/ml) for 20 to 30 min on ice, followed by two cycles of freeze-thaw. After a treatment of DNase I (10 μg/ml) over 30 min at room temperature, the lysates were centrifuged. All expressed proteins were present in the bacterial supernatant, which was run directly over a size-exclusion column (Bio-Spin P30, Bio-Rad). This first step of purification was followed by some high pressure liquid chromatography (HPLC) chromatography. The final collected fractions that proved to be fluorescent were used for our single-molecule experiments.

2.2 *Sample Preparation*

Monomers or trimers were immobilized in 2.0% agarose gels (Roche) prepared with 20 mM Hepes buffer (Gibelco).[12] These gels were melted, cooled slowly to 37°C in a water bath, mixed thoroughly with protein solution, sandwiched between two 22×22 mm glass coverslips, and allowed to cool to produce a $\sim$10-μm-thick sample.

All the coverslips used in this work were cleaned extensively before use with this sequential treatment: detergent [2% RBS (Pierce) in warm water], water, base (50% spectroscopic grade methanol saturated in KOH), water, acid (concentrated H_2SO_4), water, and spectroscopic-grade methanol, then dried with a nitrogen stream.

2.3 *Image Acquisition and Analysis*

An inverted microscope (Zeiss, Jena, Germany) equipped with a 100× oil-immersion objective (numerical aperture =1.4) was used. Samples were illuminated for 5 ms with the 514-nm line of an Ar+ laser (Coherent, Saclay, France) at a rate of 33 Hz. This excitation wavelength was chosen close to the peak absorption of citrine to minimize the excitation intensities and consequently the background noise, a key point in single-molecule detection.[10] A defocusing lens permitted us to illuminate a 20×20 μm^2 surface with an intensity of 0.9 ± 0.1 kW/cm^2. A filter set (DCLP530, HQ570/80; Chroma Technology, Brattleboro, Vermont) permitted the detection of individual fluorophores by a charge-coupled device (CCD) camera (Micromax, Roper Scientific). The total detection efficiency was $\sim$10%. The spatial distribution of the signals on the CCD originating from individual molecules was fitted to a 2-D Gaussian surface with a full-width at half-maximum of 360 ± 40 nm, given by the point-spread function of our apparatus. The number of photons emitted by a molecule or aggregate was measured in each image and was summed to get the total number of photons emitted by each structure.

3 Results and Discussion

To label the proteins, we chose the so-called citrine, a red-shifted eGFP mutant. Citrine it combines the photophysical performances of the eYFP[10,13] and a high insensitivity to changes in its environment such as pH down to 6 (Ref. 14), which can be encountered in some cellular compartments such as the endocytotic vesicles. By displaying stable luminescent properties regarding its environment, citrine is a good candidate for quantitative fluorescence measurements in cellular environments. Despite these benefits, the citrine, like all GFP mutants, suffers from blinking, which leads to the existence of an initial dark state [Fig. 1(a)].[9] We measured the distribution of the initial OFF time of 2052 purified individual citrine molecules immobilized in agarose gels. As a first approximation, the distribution was monoexponential with a characteristic time $T_{OFF}=11 \pm 1$ ms [Fig. 1(b)]. It turned out to be in the range of typical photobleaching times of GFP mutants.[10] As a consequence, the simple measurement of the intensity detected in a single image cannot reflect the number of fluorescent molecules in an aggregate. On the contrary, the distribution of the total intensity emitted by an assembly of fluorescent proteins does not depend on the characteristics of the blinking events and can be described through an analytical function. We will now present our model, then the measurements performed on a model system.

We define the mean rate of fluorescence n_{Fluo} and a mean photobleaching time τ_{bl}, and assume that they are representative of all individual citrine molecules. Following these hypotheses, the probability density function of the total count number emitted by a single citrine molecule should be a monoexponential function [Eq. (1)] characterized by N_{tot0}, defined as the mean total photon number emitted by a single citrine [Eq. (2)]:

$$p_1(N) = \exp(-N/N_{tot0})/N_{tot0} \quad (1)$$

$$\text{with } N_{tot0} = n_{Fluo}\tau_{bl}. \quad (2)$$

We validated these hypotheses by measuring the probability density function of the total number of counts detected from 2721 individual citrine molecules immobilized in agarose gels until they photobleached [Fig. 1(c)]. The experimental curve was well fitted by a monoexponential curve $\eta * p1(N)$, where η is the detection efficiency of the experimental setup, and we find $\eta \times N_{tot0} = 722 \pm 22$ counts. Interestingly, because the probability density function of the total count number emitted by a single citrine molecule is monoexponential, the mean time to obtain total photobleaching of an aggregate of molecules does not depend on the number of independent molecules present in the aggregate under identical illumination conditions.

The knowledge of $p_1(N)$ as given by Eq. (1) allowed us to derive an analytical expression for the characteristic density distribution of the total photon number $p_k(N)$ emitted by an assembly of k fluorophores. In the following discussion, we assume that the fluorescent proteins are so well separated from each other as to be considered independent emitters. More precisely, the minimal distance between citrine molecules is assumed to be greater than 5.3 nm, the Förster radius for 50% homoFRET between identical citrine molecules. The probability density function $p_k(N)$ is the convolution product of the probability function corresponding to $(k-1)$ emitters $p_{k-1}(N)$ by that of one emitter. It is thus constructed by iteration and takes the form

$$p_k(N) = (N/N_{tot0})^{k-1} \exp(-N/N_{tot0})/[(k-1)\,!\,N_{tot0}]. \quad (3)$$

Figure 2(a) presents the theoretical distributions, using Eq. (3), of the total photon number emitted by assemblies made of one, three, or five fluorescent elements. Each of them bears a characteristic form. Real systems are likely to contain a mixture of aggregates with various numbers of molecules. We thus established an experimental procedure with which to unravel the composition of the aggregates. First the parameter N_{tot0} must be measured by carrying out experiments on monomeric fluorescent proteins at the same conditions of excitation power and pH that will be used on the heterogeneous system [Fig. 1(c)]. In a second step, the distribution of the total count number corresponding to an unknown mixture of multimers (ranging for instance from monomers to pentamers) is fitted by Eq. (4):

$$p(N) = \sum_{k=1}^{5} \alpha_k (N/N_{tot0})^{k-1} \exp(-N/N_{tot0})/[(k-1)\,!\,N_{tot0}]$$

$$\text{and } \sum_{k=1}^{5} \alpha_k = 1. \quad (4)$$

We first tested the methodology numerically by using Monte-Carlo simulations based on the previous hypotheses and numerical values obtained from the measurements. We obtained the probability density of determined compositions of aggregates and applied the procedure described above on above on the distributions generated numerically. The results

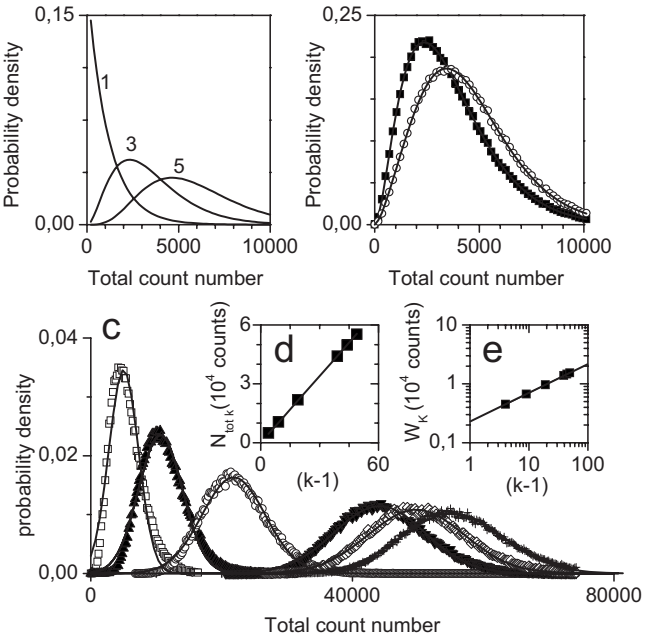

Fig. 2 (a) Theoretical probability densities functions of the total number of counts expected for pure monomers, trimers, or pentamers as indicated on the graph. (b) Simulations: Monte Carlo simulation provide the probability distributions of the total count number expected from a mixture of monomers, dimers, trimers, tetramers, and pentamers in the ratio (0%, 0%, 70%, 0%, 30%) for the open squares and (0%, 0%, 30%, 0%, 70%) for the open dots. The analysis described in the text retrieved the ratios (1%, 0%, 66%, 3%, 30%) and (0%, 1%, 27%, 0%, 70%), respectively, in very good agreement with the input parameters of the simulation. (c) Same as in (b) but for pure multimers containing a larger number of molecules (10000 multimers per simulation): 5 (□), 10 (▲), 20 (◦), 40 (▼), 45 (◇), 50 (+). The distributions are well approximated by Gaussian functions (straight lines) for aggregates containing more than 5 molecules. (d) and (e): Parameters obtained from the Gaussian fitting. In (d), N_{totk} varies linearly with $(k-1)$ and is correctly fitted by the function $I_{totk} = a \times (k-1)$, with $a = 1132 \pm 4$ when the input parameter was 1120 in the simulation. In (e), W_k varies as the square root of $(k-1)$ and can be adjusted by the relation $W_k = b \times \sqrt{(k-1)}$, with $b = 2213 \pm 5$ when 2240 was used in the simulation.

[Fig. 2(b)] confirmed the high precision of the method when it is applied to the composition of a heterogeneous population of aggregates containing a low number of elements.

The number of proteins packed in the cellular assemblies might also be high. We envisaged the case of a high number of fluorophores, k. When k is large, the distribution given by Eq. (3) can be approximated by a Gaussian function [Eq. (5)] whose width and center are related to k:

$$p_{k+1}(N) \propto \exp\left[-2\frac{(N-N_{totk})^2}{W_k^2}\right] \quad (5)$$

$$\text{with } N_{totk} = (k-1) * N_{tot0} \quad (6)$$

$$\text{and } W_k = 2 * \sqrt{(k-1)} * N_{tot0}. \quad (7)$$

The Monte Carlo simulations in the case of aggregates of purely $k = 5$, 10, 20, 40, 45, and 50 fluorophores [Fig. 2(c)]

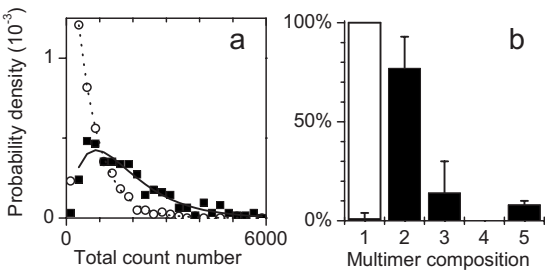

Fig. 3 (a) Measured density probability of the total number of counts corresponding to multimers of citrine (solid squares, $n=2375$). The case of monomers shown in Fig. 1(c) is also reported for comparison (open symbols). The experimental data are adjusted by the model using $N_{tot0}=722$ (straight line), which leads to the compositions of the multimers displayed in (b).

validate this approximation, since a very good agreement is found between the simulations and the analytical form for $k \geq 10$. More precisely, Gaussian fits of the simulations retrieve the widths and centers with less than 6% deviation from the input parameters [Fig. 2(d) and 2(e)]. If we now consider a mixture of large aggregates of different compositions, the center of the distribution should correspond to the average value of the number of elements gathered, whereas the width will bring information on the heterogeneity of the population of aggregates.

To test experimentally the method's reliability in the case of very small aggregates, we produced purified multimers of citrine molecules. They were constituted of monomers containing in one end the citrine and on the other end a coiled-coil domain.[11] The interaction of the coiled-coil domains is thought to lead to a multimerization of mainly three and two monomers.[11] Both domains were separated by a distance of about 20 nm, which should have ensured that the emitters behaved independently. We recorded the fluorescence emission from these multimers immobilized in agarose at low densities. The probability density of the total count number measured from individual fluorescence spots was then built, and the procedure described above applied (Fig. 3).

In the data analysis, we used the parameter $\eta \times N_{tot0}$ obtained for the pure monomers ($\eta \times N_{tot0}=722 \pm 22$ counts) [Fig. 1(c)]. Our analysis revealed that the samples were mainly constituted of dimers ($77 \pm 16\%$) and to a lesser extent of trimers ($14 \pm 16\%$). Considering that this analysis might depend on the choice of the parameter N_{tot0}, we performed the same analysis by varying N_{tot0} by 10%. The variation of the results fell within the error bars.

Our method presents a significant difference in the composition of the sample with an evaluation performed previously by electron microscopy (~50% dimers and ~50% trimers in Ref. 11). Different reasons can be given to explain this difference. First, electron microscopy provided a rough evaluation—not an *in-situ* measurement—of the sample composition because it relied on the detection of a small pool of events. Second, the multimers resulted from a coiled-coil interaction that may be deficient at the low concentrations used in single-molecule experiments due to a maturation problem. Indeed, some problems in folding and maturation of the proteins expressed after surproduction in the bacteria were encountered in some cases.[15] And even if the multimers were expected to be stabilized by covalent disulfide bonds between cysteine residues,[16,17] the dissociation time of the structure at very low concentrations, like in single-molecule experiments, was not really known. Finally, freeze and thaw cycles can produce protein denaturation, coiled-coil structure destabilization, or proteolysis of a citrine inside the trimer.

The next challenge will be to employ this procedure to get quantitative information on the composition of cellular structures. We are confident that our method can be applied to characterize mobile aggregates; nevertheless, to be effective, it will require that the structures keep stable compositions during a period of time superior to the photobleaching time of the citrine molecule. Indeed, since the method is based on the measurement of the total number of emitted photons, all the fluorescent proteins must be photobleached before the end of the experiment. In practice, most of the citrine molecules, when illuminated at their saturation intensity, will photodestruct after a few tens of milliseconds, which seems to be short enough to observe many types of biological structures. We expect that this new methodology should permit a more detailed examination of the protein content of cellular compartments.

Acknowledgments

We thank Françoise Rossignol for help in performing the citrine constructs. This work was supported by grants from the Centre National de la Recherche Scientifique, the Conseil Régional d'Aquitaine, and the Ministère de la Recherche.

References

1. G. J. Schutz, G. Kada, V. P. Pastushenko, and H. Schindler, "Properties of lipid microdomains in a muscle cell membrane visualized by single molecule microscopy," *EMBO J.* **19**(5), 892–901 (2000).
2. G. Seisenberger, M. U. Ried, T. Endress, H. Buning, M. Hallek, and C. Brauchle, "Real-time single-molecule imaging of the infection pathway of an adeno-associated virus," *Science* **294**(5548), 1929–1932 (2001).
3. M. Dahan, S. Levi, C. Luccardini, P. Rostaing, B. Riveau, and A. Triller, "Diffusion dynamics of glycine receptors revealed by single-quantum dot tracking," *Science* **302**(5644), 442–445 (2003).
4. L. Groc, M. Heine, L. Cognet, K. Brickley, F. A. Stephenson, B. Lounis, and D. Choquet, "Differential activity-dependent regulation of the lateral mobilities of AMPA and NMDA receptors," *Nat. Neurosci.* **7**(7), 695–696 (2004).
5. E. Betzig, G. H. Patterson, R. Sougrat, O. W. Lindwasser, S. Olenych, J. S. Bonifacino, M. W. Davidson, J. Lippincott-Schwartz, and H. F. Hess, "Imaging intracellular fluorescent proteins at nanometer resolution," *Science* **313**(5793), 1642–1645 (2006).
6. R. Iino, I. Koyama, and A. Kusumi, "Single molecule imaging of green fluorescent proteins in living cells: E-cadherin forms oligomers on the free cell surface," *Biophys. J.* **80**(6), 2667–2677 (2001).
7. G. S. Harms, L. Cognet, P. H. Lommerse, G. A. Blab, H. Kahr, R. Gamsjager, H. P. Spaink, N. M. Soldatov, C. Romanin, and T. Schmidt, "Single-molecule imaging of l-type Ca^{2+} channels in live cells," *Biophys. J.* **81**(5), 2639–2646 (2001).
8. K. D. Weston, M. Dyck, P. Tinnefeld, C. Muller, D. P. Herten, and M. Sauer, "Measuring the number of independent emitters in single-molecule fluorescence images and trajectories using coincident photons," *Anal. Chem.* **74**(20), 5342–5349 (2002).
9. R. M. Dickson, A. B. Cubitt, R. Y. Tsien, and W. E. Moerner, "On/off blinking and switching behaviour of single molecules of green fluorescent protein," *Nature (London)* **388**(6640), 355–358 (1997).
10. G. S. Harms, L. Cognet, P. H. Lommerse, G. A. Blab, and T. Schmidt, "Autofluorescent proteins in single-molecule research: applications to live cell imaging microscopy," *Biophys. J.* **80**(5), 2396–2408 (2001).

11. F. Coussen, D. Choquet, M. P. Sheetz, and H. P. Erickson, "Trimers of the fibronectin cell adhesion domain localize to actin filament bundles and undergo rearward translocation," *J. Cell. Sci.* **115**(12), 2581–2590 (2002).
12. B. Lounis, J. Deich, F. I. Rosell, S. G. Boxer, and W. E. Moerner, "Photophysics of *Ds*red, a red fluorescent protein, from the ensemble to the single-molecule level," *J. Phys. Chem. B* **105**(21), 5048–5054 (2001).
13. L. Cognet, F. Coussen, D. Choquet, and B. Lounis, "Fluorescence microscopy of single autofluorescent proteins for cellular biology," *C. R. Phys.* **3**, 645–656 (2002).
14. O. Griesbeck, G. S. Baird, R. E. Campbell, D. A. Zacharias, and R. Y. Tsien, "Reducing the environmental sensitivity of yellow fluorescent protein," *J. Biol. Chem.* **276**(31), 29188–29194 (2001).
15. F. Baneyx, "Recombinant protein expression in Escherichia coli," *Curr. Opin. Biotechnol.* **10**(5), 411–421 (1999).
16. K. Beck, J. E. Gambee, C. A. Bohan, and H. P. Bächinger, "The C-terminal domain of cartilage matrix protein assembles into a triple-stranded?-helical coiled-coil structure," *J. Mol. Biol.* **256**(5), 909–923 (1996).
17. V. N. Malashkevich, R. A. Kammerer, V. P. Efimov, T. Schulthess, and J. Engel, "The crystal structure of a five-stranded coiled coil in COMP: a prototype ion channel?" *Science* **274**(5288), 761–765 (1996).